

# Static and Dynamic Light Scattering from Poly(vinylbutyral) Solutions: Effects of Aggregation and Solvent Quality

C. W. Paul and P. M. Cotts\*

IBM Research, Almaden Research Center, San Jose, California 95120-6099.

Received November 20, 1986

**ABSTRACT:** Static and dynamic light-scattering data were obtained from poly(vinylbutyral) in the solvents MeOH and 1:1 and 9:1 MIBK/MeOH by volume. Concentrations spanned the dilute and into the semidilute regimes. From the static data were calculated second virial coefficients ( $A_2$ ) and  $z$ -average mean-square radii of gyration ( $\langle s^2 \rangle_z$ ). These data yield the order of solvent quality 1:1 MIBK/MeOH > 9:1 > MeOH. Static data are combined with dynamic data to determine the friction coefficients,  $f$ , for polymer/solvent mutual diffusion. In the dilute regime, values of  $f$  are greatest not in the best solvent (1:1) in which the polymer domains are largest (highest  $\langle s^2 \rangle_z$ ) but in the 9:1 MIBK/MeOH mixture. This result is attributed to the effects of inter- and intramolecular association which are most severe in the latter solvent.

## Introduction

Static light-scattering data can yield the weight-average molecular weight,  $M_w$ , the second virial coefficient,  $A_2$ , and the  $z$ -average radius of gyration,  $\langle s^2 \rangle_z$ . Dynamic light scattering gives the  $z$ -average mutual diffusion coefficient,  $D_z$ . The thermodynamic contribution to  $D_z$  can be determined from static light scattering and, thus, the polymer-solvent friction coefficient,  $f$ , evaluated through the relation<sup>1</sup>

$$D_z = \frac{M_w}{N_A f} (1 - \phi_2) \frac{\partial \pi}{\partial c} \quad (1a)$$

$$D_z = \frac{kT}{f} (1 - \phi_2) M_w \frac{Kc}{R_{0,c}} \quad (1b)$$

where  $N_A$  is Avogadro's number,  $\pi$  is the osmotic pressure,  $\phi_2$  is the polymer volume fraction,  $M_w$  is its weight-averaged molecular weight,  $c$  is its concentration in g/cm<sup>3</sup>,  $K$  is the optical constant of the light-scattering system, and  $R_{0,c}$  is the Rayleigh factor at concentration  $c$  and 0 scattering angle. The dependence of this fundamental parameter ( $f$ ) on concentration, chain expansion, and solvent chemical properties can then be investigated. The polymer used in this study, poly(vinylbutyral) (PVB), has been shown to aggregate in various solvents.<sup>2</sup> Severe aggregation dramatically increases the viscosity of semidilute solutions; however, it had no noticeable effect on the intrinsic viscosity. In this study we investigate the effects of aggregation on  $\langle s^2 \rangle_z$  and  $f$  in the dilute and into the semidilute regimes. It is found that aggregation can substantially increase the polymer-solvent friction coefficient without a corresponding increase in  $\langle s^2 \rangle_z$ .

## Equipment and Procedures

The solvents were MCB reagent grade methyl isobutyl ketone (MIBK) and EM Science glass-distilled methanol (MeOH). Poly(vinylbutyral) (PVB) with the structure shown in Figure 1 was purchased from Monsanto. This copolymer consists of 79.5 wt % acetal, 19% alcohol, and 1.5% acetate units.<sup>3</sup> A solution viscosity study of the same polymer was reported previously.<sup>2</sup> The polymer was dried in a vacuum oven at 50 °C for several days prior to use and stored in a desiccator. For all runs the highest concentration sample was prepared first. The polymer was dissolved at room temperature with the aid of a small magnetic stirring bar. The solution was then heated for 12 h at 50 °C. After cooling, solutions of lower concentration were prepared by dilution from this one initial sample.

The scattering equation for dilute polymer solutions is

$$\frac{Kc}{R_{\theta,c}} = \frac{1}{M_w P(\theta)} + 2A_2 Q(\theta) c + \dots \quad (2a)$$

where  $P^{-1}(\theta)$  is the particle-scattering function, which reflects the size and shape of the particles,  $Q(\theta)$  includes contributions from intermolecular interference at finite concentrations, and  $A_2$  is the second virial coefficient. To obtain  $Kc/R_{0,c}$  for insertion into eq 1b and for evaluation of  $M_w$  and  $A_2$ , a Chromatix KMX-6 low-angle light-scattering photometer was used. This instrument employs an angle of only  $\sim 4^\circ$ ; thus  $P^{-1}(\theta)$  and  $Q(\theta)$  are unity and eq 2a reduces to

$$Kc/R_{0,c} = 1/M_w + 2A_2 c + \dots \quad (2b)$$

The Rayleigh factor is measured directly with the KMX-6, without reference to any standards. The optical constant,  $K$ , is given by (for vertically polarized light or at low angles)

$$K = 4\pi^2 n^2 (dn/dc)^2 / N_A \lambda_0^4 \quad (3)$$

where  $n$  is the refractive index of the solvent,  $N_A$  is Avogadro's number,  $dn/dc$  is the specific refractive index increment, and  $\lambda_0$  is the wavelength of the incident light (632.8 nm). For  $n_{632.8 \text{ nm}}$  literature values of  $n_D \cong n_{632.8 \text{ nm}}$  were used.<sup>4</sup> With mixtures, we used volume-fraction-average values of  $n_{632.8 \text{ nm}}$ . Values of  $dn/dc$  were measured (using a Chromatix KMX-16) or interpolated as previously described.<sup>2</sup> The values used were 0.1562 in pure MeOH at 25 °C, 0.1284 in a 1:1 by volume mixture of MIBK and MeOH, and 0.1062 in 9:1 MIBK/MeOH. Solutions were filtered directly into the scattering cell of the KMX-6 through two 0.5- $\mu\text{m}$  Fluoropore filters (Millipore Co.). Measurements were made at room temperature while the solution flowed slowly through the cell under the action of a syringe pump. In this way dust, which appears as spikes in scattering intensity from the small ( $\sim 5 \mu\text{L}$ ) scattering volume, was easily detected and ignored in evaluating the base line of scattering intensity.

Equation 2a indicates that extrapolation of  $Kc/R_{\theta,c}$  to infinite dilution is required to obtain the  $z$ -average mean-square radius of gyration  $\langle s^2 \rangle_z$  from the particle scattering function  $P^{-1}(\theta)$ :

$$P_{\theta \rightarrow 0}^{-1}(\theta) = 1 + q^2 \langle s^2 \rangle_z / 3 + \dots \quad (4)$$

where  $q$  is the magnitude of the scattering vector

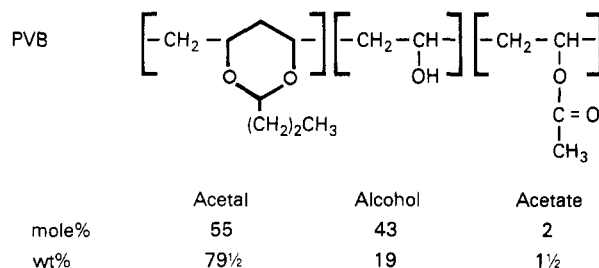
$$q = \frac{4\pi n}{\lambda_0} \sin(\theta/2) \quad (5)$$

The factor  $Q(\theta)$  in eq 2a is generally very close to unity so that eq 2a may be rewritten

$$\frac{Kc}{R_{\theta,c}} = \frac{Kc}{R_{0,c}} [1 + q^2 \langle s^2 \rangle_{z,\text{app}} / 3 + \dots] \quad (6a)$$

where

$$\langle s^2 \rangle_z = \langle s^2 \rangle_{z,\text{app}} [1 + 2A_2 M_w c + \dots] \quad (6b)$$

**Figure 1.** Structure of poly(vinylbutyral) (PVB).

$\langle s^2 \rangle_{z,\text{app}}$  at each concentration was determined by measurement of the photon count rate  $i_{\theta,c}$  at scattering angles  $\theta$  from 30° to 135° using a BI-200 SM automatic goniometer from Brookhaven Instruments

$$\langle s^2 \rangle_{z,\text{app}} = \frac{3[\partial(i_{\theta,c}^{-1})/\partial q^2]}{i_{0,c}^{-1}} \quad (7)$$

The  $\langle s^2 \rangle_z$  at each concentration was then determined by using eq 6b with the term in brackets determined by using the more precise low-angle instrument. Solutions were filtered through 0.5- $\mu\text{m}$  disposable Fluoropore filters (Millipore Co.) into 1-cm cylindrical cells which were sealed with a Teflon stopper. The temperature was controlled within  $\pm 0.1^\circ\text{C}$  and all readings were recorded at  $24.7^\circ\text{C}$ .

Dynamic light-scattering data were also obtained with the BI-200 SM by using a BI-2030 digital correlator. The correlator contains 128 data, four monitor, and eight delay channels. The last four delay channels are set at 1029–1032 times the sample time and are used to determine the measured base line. The calculated base line (infinite time value of the correlation function) is determined from the total samples and sample counts in a given experiment; these totals are stored in the monitor channels. Data were analyzed by using the method of cumulants,<sup>5</sup> which yields the equation

$$\ln \left( \frac{C(\tau)}{B} - 1 \right)^{1/2} = \ln b^{1/2} - \Gamma\tau + \mu_2\tau^2/2 - \mu_3\tau^3/6 + \dots \quad (8)$$

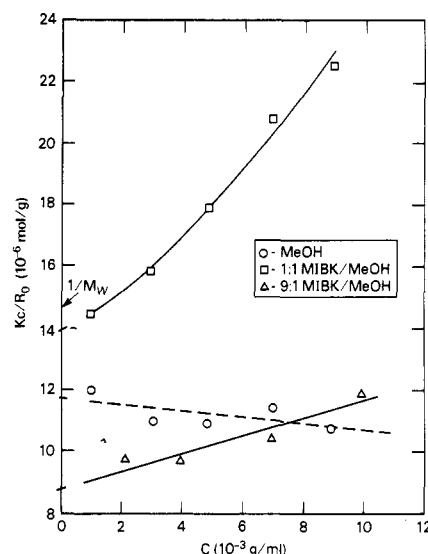
where  $C(\tau)$  is the measured autocorrelation function for a time separation  $\tau$ ,  $B$  is the base line of the correlation function,  $b$  is an optical constant,  $\Gamma$  is the first cumulant, and  $\mu_2$  and  $\mu_3$  are the second and third. Software from Brookhaven Instruments was used to evaluate the constants  $b$ ,  $\Gamma$ , and  $\mu_2$  in eq 8 (ignoring terms beyond  $\mu_2$ ) from  $C(\tau)$  and  $B$ . In these evaluations the measured base line was inserted for  $B$ . However, only data sets for which the measured and calculated base lines differed by less than 2% were accepted. Larger differences were an indication that dust contributed significantly to the correlation function and usually resulted in artificially low values of the first cumulant. The sample time ( $\Delta t$ ) was chosen based on the first cumulant so that it satisfied within 5% the relation

$$\Delta t = 2/m\Gamma \quad (9)$$

where  $m$  is the sum of data and delay channels (136). With this choice the correlation function decays to a few percent of its initial value by the 128th data channel.

## Results

**A.  $Kc/R_{0,c}$ .** Data were obtained in three solvent systems: pure MeOH, 1:1 MIBK/MeOH, and 9:1 MIBK/MeOH by volume. Plots of  $Kc/R_{0,c}$  where the subscript 0 indicates extrapolation to zero scattering angle vs.  $c$  are

**Figure 2.**  $Kc/R_{0,c}$  vs.  $c$  at room  $T$  for PVB in MeOH ( $\circ$ ), 1:1 MIBK/MeOH by volume ( $\square$ ), and 9:1 MIBK/MeOH by volume ( $\triangle$ ).

**Table I**  
Solvent Dependence of Dilute Solution Parameters

solvent	$M_{w,\text{app}}^a$ $10^3 \text{ g/mol}$	$A_{2,\text{app}}$ $10^{-4} (\text{mL mol})/\text{g}^2$	$[\eta]$ , $\text{mL/g}$	$\langle s^2 \rangle_\eta^{1/2}$ , $\text{nm}$
MeOH	85.0	-0.5	65.5	10.7
1:1 MIBK/MeOH	72.9	3.6 <sup>b</sup>	84.0	11.6
9:1 MIBK/MeOH	113.5	1.5	73.0	11.1

<sup>a</sup>  $M_{w,\text{true}} = 68500$ .<sup>2</sup> <sup>b</sup> This  $A_2$  value is about half the value we reported previously<sup>2</sup> for PVB in this solvent. We attribute this discrepancy to the fact that here we have used the limiting slope of the scattering plot to determine  $A_2$ , whereas before, data at concentrations up to  $16 \times 10^{-3} \text{ g/mL}$  were used in a linear fit to obtain  $A_2$ .

shown for all three solvents in Figure 2. According to eq 2b each plot should yield the same  $c = 0$  intercept,  $1/M_w$ . None of these plots have this intercept because of the effects of polymer aggregation and preferential solvation. The true molecular weight (see Table I) was determined in acetic acid in which the polymer showed negligible aggregation.<sup>2</sup> Aggregation reduces  $Kc/R_{0,c}$  resulting in apparent molecular weights which are too high and  $A_2$  values which are too low. Preferential solvation by one of the solvents in a mixture can alter the effective value of  $dn/dc$  used to compute  $K$  (see eq 3). Preferential solvation alters the apparent molecular weight according to<sup>6</sup>

$$M^*/M = (1 + \alpha_s(dn_0/d\phi_1)/(dn/dc)_{\phi_1})^2 \quad (10)$$

where  $M$  is the true molecular weight and  $M^*$  is the apparent value. With MeOH as solvent 1,  $\alpha_s$  is the preferential solvation coefficient of MeOH and  $dn_0/d\phi_1$  is the change in refractive index of the solvent mixture with the volume fraction of MeOH;  $(dn/dc)_{\phi_1}$  is the specific refractive index increment at constant solvent composition—previously denoted simply  $dn/dc$ . Since  $dn_0/d\phi_1$  is negative, preferential solvation by MeOH (positive  $\alpha_s$ ) lowers the apparent molecular weight. Previously reported intrinsic viscosity measurements in various MIBK/MeOH mixtures show that a 1:1 mixture of these solvents produced the maximum intrinsic viscosity.<sup>2</sup> The small discrepancy between the true and apparent molecular weights obtained in this solvent may be due to slight preferential solvation by MIBK or small amounts of aggregates. In the 9:1 mixture, preferential solvation by MeOH is expected.<sup>2</sup> This effect tends to raise the

Table II  
 $\langle s^2 \rangle_z^{1/2}$  vs. Solvent

solvent	$c, 10^{-3} \text{ g/mL}$	$\langle s^2 \rangle_z^{1/2}, \text{ nm}$
MeOH	8.95	23
	6.96	29
	4.93	29
	2.99	30
		av $28 \pm 3$
1:1 MIBK/MeOH	8.92	57
	7.99	63
	6.90	53
	5.32	59
	4.83	46
		av $56 \pm 6$
9:1 MIBK/MeOH	9.93	27
	5.93	42
	3.92	32
	2.11	31
		av $33 \pm 6$

intercept of the scattering plot. Apparently, aggregation more than offsets the effect of preferential solvation as the scattering plot for this system yields far too low an intercept. Aggregation was found to increase with the MIBK content of the solvent mixture.<sup>2</sup> The scattering plot from pure MeOH also yields an apparent molecular weight which is too high. However, it has been shown that at low enough concentrations (below the data in Figure 2) the scattering curve does turn upward.<sup>2</sup> The apparent values of  $A_2$  and  $M_w$  calculated from Figure 2 are listed in Table I. Assuming the effect of aggregation on  $A_2$  in the 9:1 solvent is minimal, the results of Table I support the previous ranking of the quality of these solvents for PVB obtained from intrinsic viscosity data<sup>2</sup>—1:1 MIBK/MeOH > 9:1 MIBK/MeOH > pure MeOH.

**B.  $\langle s^2 \rangle_z$ .** The radius of gyration can be determined from plots of  $i_{\theta,c}^{-1}$  (or  $Kc/R_{\theta}$  vs.  $\sin^2(\theta/2)$ ) by using eq 6 and 7. One such plot is shown in Figure 3. All three solvents yielded plots of similar shape. Pronounced downward curvature at low angles is often attributed to the presence of aggregates; however, excluded volume effects and large sample polydispersity may also contribute to this appearance.<sup>7</sup> Despite the index matching bath, it was difficult to obtain reliable data at  $30^\circ$  or below due to flare from the sample cell walls. The slope and intercept were therefore obtained by a linear fit of the data from  $45^\circ$  to  $90^\circ$ . Values of  $\langle s^2 \rangle_z^{1/2}$  are listed in Table II. Since the scatter in the data at any given concentration is beyond the changes in  $\langle s^2 \rangle_z^{1/2}$  due to any apparent trend with concentration, the values were averaged rather than extrapolated to  $c = 0$ . All the concentrations listed in Table II are below the overlap concentrations  $c^*$  given by

$$c^* = a/[\eta] \quad (11)$$

where  $[\eta]$  is the intrinsic viscosity and  $a$  is usually taken to be from  $1^8$  to  $3^9$ . The minimum value of  $c^*$ , setting  $a = 1$ , is obtained in the best solvent (1:1 MIBK/MeOH) where  $[\eta] = 84 \text{ cm}^3/\text{g}$  and thus  $c^* \approx 12 \times 10^{-3} \text{ g/cm}^3$ .

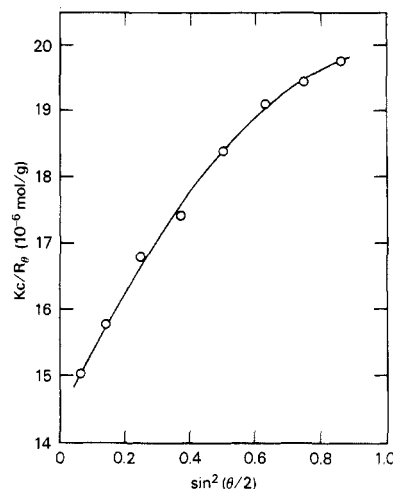


Figure 3.  $Kc/R_{\theta}$  vs.  $\sin^2(\theta/2)$  at  $24.7^\circ \text{C}$  for  $8.92 \times 10^{-3} \text{ g/mL}$  PVB in 1:1 MIBK/MeOH by volume.

Values for  $\langle s^2 \rangle_z^{1/2}$  listed in Table II may be compared with estimates obtained from the intrinsic viscosities<sup>2</sup> by the Fox-Flory equation:

$$[\eta] = \Phi \frac{\langle r^2 \rangle_z^{3/2}}{M} \quad (12)$$

with  $\Phi = 2.5 \times 10^{23}$  and  $M = M_w = 68500$ .<sup>2</sup> Values obtained for  $\langle s^2 \rangle_z^{1/2}$  where

$$\langle s^2 \rangle_z^{1/2} = (\langle r^2 \rangle_z/6)^{1/2} \quad (13)$$

are listed with  $[\eta]$  in Table I. Comparison with  $\langle s^2 \rangle_z^{1/2}$  in Table II obtained by light scattering shows a large discrepancy.

Measurements in the 1:1 solvent mixture gave values of  $\langle s^2 \rangle_z^{1/2}$  which were much larger than in the other two solvents. Although the second virial coefficient  $A_2$  is largest in this solvent mixture, the apparent expansion of the chain in this solvent is substantially larger than expected. The expansion factor  $\alpha_s$  where

$$\alpha_s^2 = \langle s^2 \rangle / \langle s^2 \rangle_0 \quad (14)$$

may be estimated from the intrinsic viscosities by assuming

$$\alpha_s^3 \approx \alpha_\eta^3 \equiv [\eta]/[\eta]_0 \quad (15)$$

and that the polymer chain has nearly unperturbed dimensions in MeOH where  $A_2 \approx 0$ . Using these relations, we find that expansion in the 1:1 solvent should be small, i.e.,

$$\alpha_s = \langle s^2 \rangle^{1/2} / \langle s^2 \rangle_0^{1/2} = 1.10$$

rather than 2 as measured experimentally.

Several experiments were conducted to gauge the influence of aggregation on  $\langle s^2 \rangle_z$ . These experiments are summarized in Table III. It was found that heating and then cooling reduced the scattering intensity, thus raising  $Kc/R_{\theta,c}$  as expected for disaggregation. This effect was most severe in the 9:1 MIBK/MeOH solvent mix (25% decrease in  $R_{\theta}$ ), indicating that aggregation is most severe

Table III  
 Effects of Heat Treatment on  $R_{\theta}$  and  $D_z$

solvent	$c, 10^{-3} \text{ g/mL}$	heat treatment	% change in $R_{\theta}^a$ ( $t, h$ after heating)	% change in $D_z^a$ ( $t, h$ after heating)
MeOH	2.99	$3/4 \text{ h } 50^\circ \text{C} + 1 \text{ h } 70^\circ \text{C}$	$\sim 0\%$ ( $1/4$ ), $\sim 0\%$ (4)	$\sim 0\%$ (4)
1:1 MIBK/MeOH	16.29	$3.5 \text{ h } 50^\circ \text{C}$	$-3\%$ , ( $1/4$ ), $\sim 0\%$ (27)	$+3\%$ ( $1/4$ )
	2.89	$3/4 \text{ h } 50^\circ \text{C} + 1 \text{ h } 70^\circ \text{C}$	$-1\%$ (7)	
9:1 MIBK/MeOH	3.92	$3/4 \text{ h } 50^\circ \text{C} + 1 \text{ h } 70^\circ \text{C}$	$-25\%$ (1), $-22\%$ (3), $-16\%$ (19)	$+10\%$ (1)

<sup>a</sup> The percent change represents the difference between values obtained before heating and  $t$  hours after heat treatment. The number of hours is given in parentheses beside each percent change. The percent change in  $R_{\theta}$  and  $D_z$  was nearly the same at all angles.

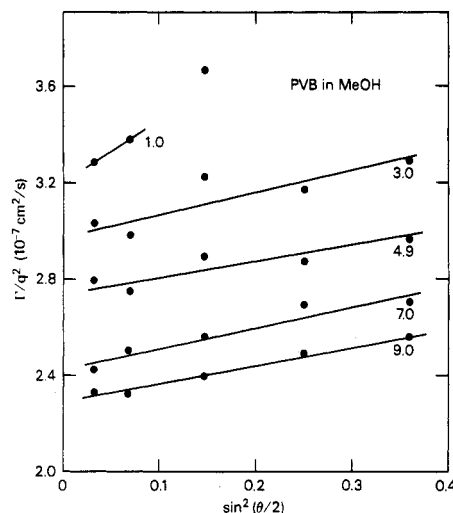


**Figure 4.**  $\Gamma/q^2$  vs.  $\sin^2(\theta/2)$  at 24.7 °C for PVB in MeOH at the concentrations indicated at the right edge of each line segment (units of  $10^{-3}$  g/mL).

in this solvent. After 19 h the scattering intensity recovered about one-third of its initial drop. The percent reduction in  $R_\theta$  was only slightly higher at larger angles. Consequently scattering plots of  $Kc/R_{\theta,c}$  vs.  $\sin^2(\theta/2)$ , such as that shown in Figure 3, retained their shape after heating but were displaced upward. The insensitivity of the parameter  $\langle s^2 \rangle_z/M_{w,app}$  obtained from the initial slope to aggregation has also been observed with cellulose acetate solutions.<sup>11</sup> This fact also helps explain the insensitivity of the intrinsic viscosity to aggregation which has been observed with our systems<sup>2</sup> and by others.<sup>7,11,12</sup> Since typically<sup>13</sup>  $[\eta] \propto \langle s^2 \rangle^{3/2}/M$ , the offsetting effects of aggregation on  $\langle s^2 \rangle$  and  $M$  serve to keep  $[\eta]$  relatively unaffected. The strong contribution of the aggregated species to  $\langle s^2 \rangle_z$  measured by static light scattering is responsible for the large change in  $\langle s^2 \rangle_z$  with heat treatment. The observed disaggregation by heat treatment is consistent with previous work<sup>10</sup> which demonstrated that heat treatment of dilute solutions was sufficient to remove nearly all the aggregation temporarily. For example, heat treatment of solutions in several solvents which had yielded large apparent  $M_w$  (including MeOH) resulted in agreement of  $M_w$  with that obtained in acetic acid, where no evidence of aggregation was observed. Heat treatment of acetic acid solutions did not change the measured  $M_w$ .

**C.  $D_z$ .** The light-scattering autocorrelation experiment yields the first and second cumulants,  $\Gamma$  and  $\mu_2$ , of eq 8. The  $z$ -average diffusion coefficient

$$D_z \equiv \frac{\sum_i w_i M_i D_i}{\sum_i w_i M_i} \quad (16)$$

is obtained from the first cumulant, where  $w_i$  is the mass of component  $i$  and  $M_i$  is its molecular weight. Calculation of  $D_z$  requires extrapolation of  $\Gamma/q^2$  to  $\theta = 0$ . The angular dependence of the reduced first cumulant,  $\Gamma/q^2$ , in the solvent MeOH is shown at several concentrations in Figure 4. Here  $q$  is the magnitude of the scattering vector; see eq 5. Plots similar to Figure 4 were also obtained with the solvents 1:1 and 9:1 MIBK/MeOH. The intercepts of these plots yield values of  $D_z$  at different concentrations. The results for all three solvents are shown in Figure 5. Below  $c^*$  (see eq 11),  $D_z$  represents the mutual diffusion coefficient for translational diffusion of the polymer. Above  $c^*$  cooperative diffusion of portions of the polymer chains may be detected at the short sample times used in

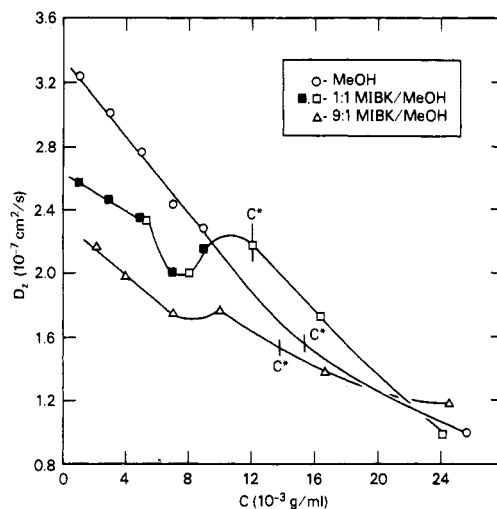


**Figure 5.**  $D_z$  vs.  $c$  at 24.7 °C for PVB in MeOH (○), 1:1 MIBK/MeOH by volume (■ and □, two different sets of experiments), and 9:1 MIBK/MeOH by volume (△). The chain overlap concentrations,  $c^*$ , were estimated from eq 11 using  $\alpha = 1$ .

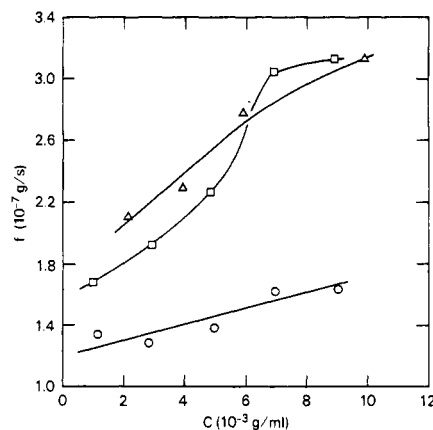


**Figure 6.**  $f$  vs.  $c$  at 24.7 °C for PVB in MeOH (○), 1:1 MIBK/MeOH by volume (□), and 9:1 MIBK/MeOH by volume (△).

this study.<sup>8,14</sup> Setting  $\alpha = 1$  in eq 11,  $c^*$  has been evaluated for each solvent and is indicated by a vertical dash on the curves in Figure 5. The most unusual features in Figure 5 are the sharp minimum and maximum in the curve for the 1:1 solvent well before the overlap concentration should have been reached. The curve for the 1:1 mix superimposes the data of two separate groups of solutions which both showed this behavior. The results shown in Figure 5 are more meaningfully interpreted by using eq 1b and the data of Figure 2 to calculate the friction coefficients,  $f$ , for polymer-solvent diffusion. In calculating  $f$  from eq 1b the apparent weight-average molecular weight was used for  $M$  to avoid introducing any errors in  $K$  due to preferential solvation. Values of  $f$  are shown vs. concentration for all three solvents in Figure 6. These results are not significantly influenced by differences in solvent viscosity. MeOH and 9:1 MIBK/MeOH have virtually the same viscosity and the viscosity of the 1:1 mixture is only 1.3% lower.<sup>2</sup> The complicated shapes observed in Figure 5 for the concentration dependence of  $D_{z,c}$  are due to the competing effects of thermodynamic and hydrodynamic factors as well as any dependence of the extent of aggregation on concentration. For all three solvents  $f$  is a monotonically increasing function of concentration. The initial portion of these curves can be fitted to a linear equation of the form

$$f = f_0(1 + k_f c + \dots) \quad (17)$$

**Table IV**  
Constants of Equation 17 vs. Solvent

solvent	$f_0, 10^{-7} \text{ g/s}$		$k_f, \text{ mL/g}$	
	exptl	theory	exptl	theory
MeOH	1.2	0.9	42	46
1:1 MIBK/MeOH	1.5	1.7	100	173
9:1 MIBK/MeOH	1.7	1.0	107	129

**Table V**  
 $\rho \equiv \langle s^2 \rangle_z^{1/2} \langle 1/R_H^D \rangle_z$  vs. Solvent

solvent	$\langle 1/R_H^D \rangle_z^{-1}, \text{ nm}$	$\rho$	$\rho_{\text{COR}}$
MeOH	12	$2.3 \pm 0.2$	1.0
1:1 MIBK/MeOH	16	$3.6 \pm 0.4$	1.5
9:1 MIBK/MeOH	17	$2.0 \pm 0.4$	0.9

The constants obtained from these fits are given in Table IV along with theoretically predicted values. The effective hydrodynamic radius, ( $R_H \equiv \langle 1/R_H^D \rangle_z^{-1}$ ) was calculated from the limiting diffusion coefficient at infinite dilution by using the Stokes-Einstein relation:

$$D_z^0 = \left( \frac{kT}{6\pi\eta_s} \right) \langle 1/R_H^D \rangle_z \quad (18)$$

Values for  $\langle 1/R_H^D \rangle_z^{-1}$  are listed in Table V. Aggregation has a smaller effect on  $D_z$  than  $R_\theta$ . Heat treatment of a solution of PVB in 9:1 MIBK/MeOH produced only a 10% increase in  $D_z$  but a 25% reduction in  $R_\theta$  (see Table III). Heat treatment with MeOH as the solvent produced no change in  $D_z$ ; in 1:1 MIBK/MeOH only a 3% increase was observed.

## Discussion

The various experimental parameters can be interpreted by considering the extent to which they are affected by the presence of a small weight fraction of large aggregates. Certain parameters, i.e.,  $\langle s^2 \rangle_z$ ,  $M_{w,\text{app}}$ , and  $M_z/M_w$  determined by GPC with a light-scattering detector (GPC-LS) are quite sensitive to the presence of large aggregates as evidenced by their anomalously large values and by their dependence on solvent and heat treatment. Conditions under which the latter two parameters may nearly reflect the nonaggregated species were discussed previously.<sup>2,10</sup> Other parameters such as  $[\eta]$ ,  $\langle 1/R_H^D \rangle_z^{-1}$ , and  $M_z/M_w$  determined by GPC alone are relatively insensitive to the presence of a small fraction of large aggregates and tend to reflect the structure of the nonaggregated species. These parameters are nearly independent of heat treatment even in solvents exhibiting large apparent  $M_w$  and bimodal chromatograms obtained by GPC-LS. In addition,  $[\eta]$  appears to vary little whether or not the solvent is one in which substantial aggregation is present. Comparison of experimental parameters discussed below is divided into two sections, one addressing parameters sensitive to aggregation and one where parameters are insensitive and/or aggregation is minimized by choice of solvent or heat treatment.

**A. Parameters Sensitive to Aggregation.** Values of  $\langle s^2 \rangle_z^{1/2}$  (Table II) are much larger than  $\langle s^2 \rangle_\eta^{1/2}$  (Table I). We attribute this difference to the large apparent polydispersity of these samples, due in part to the presence of aggregated species. Although  $M_w/M_n$  is approximately 3 by GPC, the chromatograms showed a higher molecular weight tail and  $M_z/M_w = 2.7 \pm 1$ , substantially higher than the 1.7 expected for a Schulz distribution with  $M_w/M_n = 3$ . Earlier work<sup>10</sup> using a light-scattering detector (GPC-LS) showed that aggregated species contributed strongly to this high molecular weight region, and values for  $M_z/M_w \approx 4-6$  were commonly observed. Chromatograms obtained

by GPC-LS were bimodal with a large peak in the high molecular weight portion of the distribution. The amplitude of this peak was very sensitive to heat treatment of the sample solution and to filtration. In contrast, the chromatograms obtained with the refractive index detector alone (GPC) were monomodal, with only a small shoulder in the region of the high  $M$  peak in the GPC-LS chromatogram, and were little affected by heat treatment or filtration. The light-scattering detector is very sensitive to the high molecular weight portion of the distribution and permits detection of large species which may be present in nearly negligible weight fraction. Determination of polydispersity using GPC alone minimizes the contribution from the aggregated species, while GPC-LS is the technique most sensitive to the presence of aggregated material.<sup>10</sup> The determinations of the radius gyration by light scattering and from the intrinsic viscosity are consistent if  $M_z/M_w = 6$ . We estimate  $M_w/M_n$  assuming a log normal distribution which is similar to that obtained experimentally by GPC:

$$w(M_i) = \frac{1}{\beta\pi^{1/2}} \frac{1}{M_i} \exp \left[ -\left( \frac{1}{\beta} \ln \frac{M_i}{M_0} \right)^2 \right] \quad (19)$$

where  $M_w = M_0 \exp(\beta^2/4)$  and  $M_w/M_n = \exp(\beta^2/2) = M_z/M_w$ , etc. The viscosity average  $M_\eta$

$$M_\eta = [\sum w_i M_i^a]^{1/a} \quad (20)$$

is then estimated for  $\beta = 1.5$  (i.e.,  $M_w/M_n = 3$ ) and  $a = 0.5$ . This yields  $M_w/M_\eta = 1.4$ . For  $M_z/M_w = 4-6$ , as was observed with the light-scattering detector,  $M_z/M_\eta = 7 \pm 1.4$ , which is consistent with the light-scattering and viscosity results. We believe the smaller values of  $M_z/M_w = 3$  obtained by GPC alone are due to loss of sensitivity of the detector at the high- $M$  portion of the distribution. It should be noted that both GPC and GPC-LS measurements were carried out in tetrahydrofuran, which is not a solvent used for the light-scattering measurements. Since the degree of aggregation varies with solvent, estimation of  $M_z/M_\eta$  from these data is only a qualitative measure of the contribution of aggregated species to  $\langle s^2 \rangle_z$ .

Values of  $\langle s^2 \rangle_z$  in the 1:1 solvent mixture were much larger than in the other two solvents, whereas an increase of only 20% is expected based on intrinsic viscosity results. Correction of the estimated  $\alpha_s$  for polydispersity assuming

$$\alpha_s^2 \propto M^\nu \quad (21)$$

with  $0 \leq \nu \leq 1/5$  yields

$$\alpha_{s,z} \approx 1.4$$

The experimental value is much larger, approximately 2. Increased population of aggregates could contribute to a large  $\langle s^2 \rangle_z^{1/2}$ ; however, the aggregation increases with MIBK content and the  $\langle s^2 \rangle_z^{1/2}$  is smaller in the 9:1 solvent mixture. The increased apparent expansion may be due to a pseudobranched structure of the aggregates which dominate the high molecular weight end of the distribution. The increased number of segmental contacts present in branched structures leads to an increase in  $\alpha_s$  in comparison to that observed for linear chains.

Information about polymer structure may often be obtained from the dimensionless parameter  $\rho \equiv \langle s^2 \rangle_z^{1/2} \langle 1/R_H^D \rangle_z$  listed in Table V which should be less sensitive to errors in absolute molecular weight determination.<sup>19</sup> This parameter increases with solvent quality and polydispersity but decreases with branching. Theory predicts<sup>17</sup> that  $\rho$  will vary from 1.51 to 1.86 as the solvent goes from a  $\theta$  to a good one for a monodisperse polymer. An increase of 15%

in  $\rho$  is predicted as  $M_w/M_n$  goes from 1 to 2 for a polymer with a Zimm-Schulz distribution in a  $\Theta$ -solvent. Values for  $\rho$  calculated directly from the experimental quantities, with no correction for polydispersity, are listed in Table V and are all larger than theoretically predicted values. Theories of  $\rho$  for polydisperse polymer samples assume a most probable distribution with  $M_z/M_w = 1.5$ . For samples here, where  $M_z/M_w$  is approximately 5, we can easily expect  $\rho$  to be much higher. These uncorrected values for  $\rho$  are dominated by the high molecular weight portion of the distribution, which contains contributions from the aggregated species.

**B. Parameters Least Sensitive to Aggregation.** The hydrodynamic radius  $R_H$  listed in Table V is expected to be much less sensitive to a small fraction of aggregates than  $\langle s^2 \rangle_z$ . Determination of  $R_H$  by dynamic light scattering using the method of cumulants emphasizes contributions from smaller species. However, comparison of  $R_H$  in Table V with  $\langle s^2 \rangle_z^{1/2}$  in Table I suggests that  $R_H$  determined by dynamic light scattering may be more affected by aggregation than  $[\eta]$ , at least for solvents containing large amounts of MIBK where aggregation becomes severe.

The intercept,  $f_0$ , of eq 17 is predicted to increase with the chain dimensions in the manner<sup>17</sup>

$$f_0 = 6^{1/2} \eta_s P \langle s^2 \rangle^{1/2} \quad (22)$$

where  $\eta_s$  is the solvent viscosity and  $P$  is assumed to be a universal constant with the value 5.11 obtained for the Kirkwood Riseman model with infinite hydrodynamic interaction. The measured value for  $\langle s^2 \rangle_z^{1/2}$  must be corrected to a weight average to compare the measured  $f_0$  with that predicted by eq 22 above. Although the infinite-dilution limit of the mutual diffusion coefficient determined by the method of cumulants is a  $z$ -averaged quantity (see eq 16) it is inversely related to the hydrodynamic radius,  $R_H$  (or, equivalently,  $M^{1/2}$ ), and thus is most closely related to the diffusion coefficient expected for a monodisperse polymer with  $M = M_w$ . In contrast, the  $z$ -averaged mean-square radius of gyration measured by static light scattering,  $\langle s^2 \rangle_z$ , is most closely related to  $\langle s^2 \rangle$  expected for a monodisperse polymer with  $M = M_z$ . Using  $M_z/M_w = 5$  as discussed above, we calculate  $\langle s^2 \rangle_w^{1/2}$  by using  $\langle s^2 \rangle_z^{1/2}$  from Table II; the results for  $f_0$  are shown in Table IV. The agreement is poor, which we attribute to the difficulty encountered in obtaining accurate values of  $\langle s^2 \rangle_z$  from static light scattering, which is strongly affected by the presence of aggregates. The most critical discrepancy is the prediction of a slower diffusion in the 1:1 solvent in comparison to the other two, based on the substantially larger value for  $\langle s^2 \rangle_z$  measured in this solvent. In contrast, the measured diffusion in this solvent was faster than in the 9:1 solvent. Theory due to Yamakawa<sup>18</sup> can be used to predict the concentration dependence of  $f$

$$k_f = 1.2 A_2 M + \frac{N_A V_m}{M} \quad (23)$$

where

$$V_m = \frac{4}{3} \pi R_H^3$$

Apparent values of  $A_2$  and  $M_w$  were used in determining the predicted values of  $k_f$  given in Table IV. Application of these theories to a polymer exhibiting aggregation is very tenuous, particularly for a parameter that is concentration

dependent since the extent of aggregation may well increase with concentration. The qualitative agreement between theoretical and measured values shown in Table IV is additional evidence that these parameters are less sensitive to the presence of a small weight fraction of large aggregates than those such as  $M_{w,app}$  and  $\langle s^2 \rangle_z$  discussed above.

Correction of  $\langle s^2 \rangle_z^{1/2}$  to a weight average, as was used above to calculate  $f_0$ , allows an estimation of  $\rho$  which may be least affected by the large polydispersity:

$$\rho_{COR} \equiv \langle s^2 \rangle_w^{1/2} \langle 1/R_H^D \rangle_z \quad (24)$$

Values for  $\rho_{COR}$  listed in Table V are close to unity for MeOH and the 1:1 solvent mixture. While this is significantly less than the 1.5 predicted for monodisperse linear polymer chain in  $\Theta$ -solvents, it is close to the experimental values of  $\sim 1.2$  observed for several narrow distribution polymers under  $\Theta$ -conditions.<sup>19</sup> The higher value for  $\rho_{COR}$  in the 1:1 solvent mixture is consistent with the substantially larger  $A_2$  observed in this solvent.

## Summary and Conclusions

Diffusion is fastest and the root-mean-square radius of gyration ( $\langle s^2 \rangle_z^{1/2}$ ) is smallest in MeOH, the poorest solvent. The computed friction coefficients in MeOH are also lowest and least concentration dependent. In 1:1 MIBK/MeOH, the best solvent,  $\langle s^2 \rangle_z^{1/2}$  is larger than in MeOH, as expected; the limiting friction coefficient is greater and  $f$  increases more than twice as rapidly with concentration. The 9:1 MIBK/MeOH solvent mixture is a poorer one for PVB than the 1:1 mix and the value of  $\langle s^2 \rangle_z^{1/2}$  is smaller as expected. However, diffusion is slowest in the 9:1 mix and the friction coefficient increases most rapidly with concentration in this solvent. Two phenomena which may contribute to these results are inter- and intramolecular association. Association is by far most severe in the 9:1 MIBK/MeOH solvent.

## References and Notes

- (1) Yamakawa, H. *Modern Theory of Polymer Solutions*; Harper and Row: New York, 1971; p 262.
- (2) Paul, C. W.; Cotts, P. M. *Macromolecules* **1986**, *19*, 692.
- (3) The alcohol content was determined by Monsanto. The weight fraction of acetal was determined by: Sachdev, K.; Khojasteh, M.; Shear, S., of IBM, East Fishkill, New York.
- (4) Elias, H. G. In *Polymer Handbook*, 2nd ed.; Brandrup, J., Immergut, E. H., Eds.; Wiley: New York, 1975; p VII-23.
- (5) Brown, J. C.; Pusey, P. N.; Dietz, R. J. *Chem. Phys.* **1975**, *62*, 1136.
- (6) Strazielle, C. In *Light Scattering from Polymer Solutions*, Huglin, M. B., Ed.; Academic: New York, 1972; p 652.
- (7) Kratochvil, P. In *Light Scattering from Polymer Solutions*; Huglin, M. B., Ed.; Academic: New York, 1972; p 333.
- (8) Chang, T.; Yu, H. *Macromolecules* **1984**, *17*, 115.
- (9) Martin, J. E. *Macromolecules* **1984**, *17*, 1279.
- (10) Cotts, P. M.; Ouano, A. C. In *Microdomains in Polymer Solutions*; Dubin, P., Ed.; Plenum: New York, 1985; p 101.
- (11) Tanner, D. W.; Berry, G. C. *J. Polym. Sci., Polym. Phys. Ed.* **1974**, *12*, 941.
- (12) Chiang, R.; Stauffer, J. C. *J. Polym. Sci., Polym. Phys. Ed.* **1967**, *5*, 101.
- (13) Flory, P. J. *Principles of Polymer Chemistry*; Cornell University Press: Ithaca, NY, 1953; p 611.
- (14) Hwang, D.; Cohen, C. *Macromolecules* **1984**, *17*, 1679.
- (15) Nose, T.; Chu, B. *Macromolecules* **1979**, *12*, 590.
- (16) Roots, J.; Nyström, B. *Macromolecules* **1980**, *13*, 1595.
- (17) Mandelkern, L.; Flory, P. J. *J. Chem. Phys.* **1952**, *20*, 212.
- (18) Yamakawa, H. *Modern Theory of Polymer Solutions*; Harper and Row: New York, 1971; p 314.
- (19) Burchard, W. R. *Adv. Polym. Sci.* **1983**, *48*, 1.